IAC-19-B1.3.8

Tunable mid-wave infrared spectral filters based on Ge$_x$Sb$_y$Te$_z$ for multispectral imaging

Hyun Jung Kim[a]*, Matthew Julian[a,b], Calum Williams[c], Scott Bartram[d]

[a] *National Institute of Aerospace, 100 Exploration Way, Hampton, VA 23693 US*
[b] *Department of Electrical and Computer Engineering, University of Virginia, Charlottesville, VA 22904 US*
[c], *Department of Physics, Cavendish Laboratory, University of Cambridge, Cambridge, CB3 0HE, UK*
[d] *NASA Langley Research Center, Hampton, VA 23666, US*

* Corresponding Author, *hyunjung.kim@nasa.gov*

Abstract

The mid-wave infrared (MWIR) spectrum contains a wealth of invaluable information including the spectral 'fingerprint' of many chemical species and has applications in remote sensing and astronomical imaging. Traditionally, filtering for the MWIR is achieved by means of passive multilayer interference (dichroic) filters, Fabry-Perot-based micro-electro-mechanical system (MEMS) filters, liquid crystal tunable filters, and focal plane array (FPA) filters. For accurate multispectral imaging applications, these approaches suffer from various limitations such as: having moving parts; exhibiting slow response times, and; having limited spectral bandwidth / resolution. Recently, there has been significant interest toward 'active' spectral imaging technologies, whereby the ability to provide electrically tunable narrowband filtering—spanning the entire MWIR—is highly desirable. In this work we introduce a new spectral imaging technology, namely actively tunable optical transmission filters using the phase-change material (PCM) Ge$_x$Sb$_y$Te$_z$ (GST). The GST exhibits a large, reversible change in its refractive index across the MWIR upon a phase transition (from amorphous to crystalline). This refractive index modulation governs the filter's optical characteristics. Through an optical stimulus or applied voltage—which changes the GST state from amorphous to crystalline—one can actively tune the filter with MHz speed. We incorporate GST into optimized guided mode resonance (GMR) and plasmonic nanohole array (PNA) device architectures, enabling <10nm spectral resolution and tunable operation across 3~5µm. Our proposed PCM-MWIR filter will be able to extract the maximum amount of 'useful' information within the atmosphere for remote Earth sensing measurements at operational speeds orders of magnitude faster than current airborne-based sensors. Moreover, it may enable affordable SmallSat-based MWIR instrumentation which is complimentary to other observation systems. The MISSE (Materials International Space Station Experiment-Flight Facility) experiment has been proposed as a testbed for a PCM-based tunable MWIR filter module to allow exposure of the module to the low Earth orbit space environment. This will provide valuable data regarding the robustness of the filter to withstand the radiation and atomic oxygen environment and allow assessment of the technology for use in space applications.

Keywords: Tunable filter, mid-wave infrared (MWIR), active filter, phase change material, GeSbTe, MHz speed

Nomenclature
Ge Germanium
ZnSe Zinc Selenide
H$_2$O water (vapor)
CH$_4$ methane
λ wavelength
n refractive index of the guiding layer
CaF$_2$ calcium fluoride
KHz kilohertz
MHz megahertz
CO / CO$_2$ Carbon monoxide and Carbon dioxide
ns Nanosecond
ε_m permittivity of metal film
ε_d permittivity of surrounding dielectric

l, j integer
W watt

Acronyms/Abbreviations
MWIR Mid-wave Infrared
FPA Focal Plane Array
MEMS Micro-Electro-Mechanical Systems
PCM Phase Change Material
GST Ge$_x$Sb$_y$Te$_z$; Germanium Antimony Telluride
GMR Guided Mode Resonance
PNA Plasmonic Nanohole Array
MISSE Materials International Space Station Experiment
DIAL Differential Absorption LIDAR
LIDAR Light Detection and Ranging

CFD Computational Fluid Dynamics
SLS Space Launch System
PIFS Plume Induced Flow Separation
EM-1 Exploration Mission-1
SWaP Size, Weight, and Power
LaRC Langley Research Center
PRAM Phase Change Random Access Memory
FT-IR Fourier-Transform Infrared
FWHM Full Width at Half Maximum
ISS International Space Station
FDTD Finite-difference Time Domain
Nd:YAG Neodymium-doped Yttrium Aluminium Garnet
SEM Scanning Electron Microscope
CIF Center Innovation Fund
SD Science Directorate
IRAD Internal Research and Development
FY Fiscal Year
LEO Low Earth Orbit
UV Ultraviolet

1. Introduction

The mid-wave infrared (MWIR) spectrum contains a wealth of invaluable information: from the spectral 'fingerprint' of many chemical species, with applications in remote sensing, to radiant thermal signatures, utilized in astronomical and military imaging systems as shown in Figure 1 [1-3]. Traditionally, filtering for the MWIR is achieved by means of passive multilayer interference (dichroic) filters, allowing for an extremely narrow filtering bandwidth. Image sensors in the MWIR typically utilize focal plane array (FPA) technology, analogous to pixel arrays in the visible in that they consist of solid-state sensors with overlaid filter mosaics used to spectrally discriminate the input light at specific spatial intervals. Depending on the wavelength range, detectors fabricated from a specific semiconductor material (e.g. InSb for MWIR applications), are covered by a filter mosaic baseplate in order to detect independent wavelengths (spectral bands). Additionally, other, more advanced device types can be utilized, such as quantum-well FPAs, however the fabrication complexity and cost significantly increase [4]. MWIR FPAs and filters are generally analogous in operation to their visible spectrum counterparts, but typically require exotic material combinations (such as Ge or ZnSe) as conventional (visible spectral) materials, which are transparent in the visible, are generally opaque in the MWIR. Recently, there have been developments toward 'smart' spectral imaging technologies; whereby the ability to provide electrically tunable narrowband filtering—spanning the entire MWIR—is highly desirable. Common technological approaches include Fabry-Perot-based micro-electro-mechanical systems (MEMS) [5], piezoelectric devices [6], and liquid crystal tunable filters

[7]. However, these approaches suffer from various limitations, such as: having moving parts, are complex to manufacture, require high switching voltages, have slow response times and limited spectral bandwidth / resolution. For accurate next-generation MWIR spectral imaging applications, the ability to extract the maximum amount of information with high-resolution (<10 nm), rapid tuning speeds (>MHz), with reduced size and mass, is paramount. Phase change materials (PCMs) offer the advantages of fast switching speed (nanosecond read/write speeds), high switching robustness (potentially up to 10^{15} cycles), and scaling potential. This presents an important and highly relevant ultrafast and active tuning optical device applications for combining PCMs with integrated known passive optical device design [8,9]
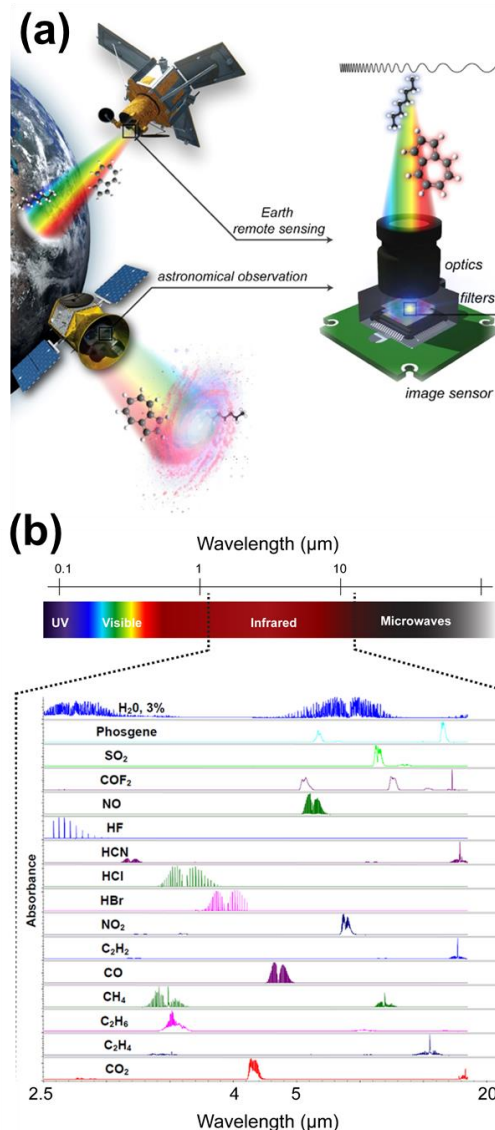
Figure 1. IR spectral fingerprint. *(a) Schematic diagram of the tunable filter applications in space exploration and science mission programs. (b) Atmospheric absorbance as a function of wavelength across the infrared (2.5 ~20 μm).*

1.1 Active tunable filter for H2O and CH4 DIAL system

A deeper understanding of how clouds will respond to a warming climate is one of the outstanding challenges in climate science [10]. Water vapor (H_2O) and methane (CH_4) are the most dominant greenhouse gases and play a vital role in both the climate and weather. Uncertainties in the response of clouds, and particularly shallow clouds, have been identified as the dominant source of the discrepancy in model estimate of equilibrium climate sensitivity. By combining DIAL profiles of H_2O, CH_4, aerosols, and clouds, the community gains a deeper understanding of a boundary layer processes (shallow clouds, shallow and deep convection, convective aggregation, arctic mixed phase clouds, etc.) and weather and dynamics (genesis and intensification of hurricanes, land-atmosphere feedbacks, etc.) [11]. The active tunable filter would be a central component for climate models; providing for more accurate H_2O and CH_4 profiles from an affordable instrument (high altitude airborne platforms or SmallSat-based) that compliment other observation systems.

1.2 Tunable filter for core stage thermal imaging of the EM-1 SLS

On the core stage of the EM-1 (Artemis 1) SLS, a super-heavy thermal protection system has been applied to protect the engine [12]. A temperature deviation exists between the CFD and the wind tunnel testing results, and wind tunnel testing has difficulty scaling up the measurements to realistic flight conditions. An accurate temperature measurement of the surface of the rocket core booster stage and the Plume Induced Flow Separation (PIFS), flames climbing the rocket body, are important to reduce the weight of the heat shield system. Currently, filter wheels (operating at <kHz speeds) are adapted for multiple narrow band MWIR signals—2~5 µm for H_2O and CO / CO_2 plume emission—using several passive narrowband filters. The motorized filter wheel is bulky and requires numerous mechanical components to operate, along with motors, and extensive power electronics. Moreover, the wheel provides discrete transmission windows, thus sampling the target spectral information at only several points. An idealistic alternative would provide actively tunable, all solid-state, narrowband, high frequency (>MHz) MWIR filtering. This filter would greatly improve key component metrics of size, weight, and power (SWaP) of the mission.

2. Material and technical approach

In this work we study the performance of a novel, narrow bandwidth, actively tunable optical transmission filter operating across 2~5µm by utilizing the material $Ge_xSb_yTe_z$ (GST).

GST is a phase change material (GST-PCM) exhibiting a large, reversible change in its refractive index upon phase transition (crystallization) [13]. This occurs rapidly (MHz) when the GST film is heated above a critical temperature, determined by its stoichiometry, generally near 150 °C [14]. It is a widely known as a computer memory material, with nanosecond read/write speeds. Recently, metamaterials integrated with PCMs have allowed greater control of light across nanoscale dimensions with proposed optical device applications including spectral filters, waveguides, displays, and beam-steering [8-9,15-16]. Critical to this work is the large change in GST refractive index: n = 3.7 (amorphous), n = 6.0 (crystalline) at λ= 2µm, and large modulation across the entire MWIR [Figure 2].
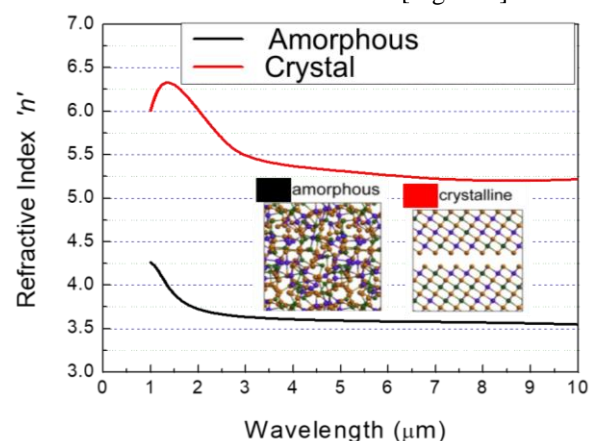

Figure 2. *Complex refractive index data of the GST films deposited on CaF_2 substrate measured via RC2 and infrared variable-angle spectroscopic ellipsometry (J.A. Woollam). Spectral analysis was performed at wavelengths from 1µm to 10µm with 55° to 75° angles of incidence by 10° step.*

3. Design and demonstration of GST-based tunable transmission filters

The refractive index modulation of the GST-PCM across the MWIR upon a phase transition, (amorphous and crystalline) provides the core of our designed filter's optical characteristics. We incorporate GST into conventionally passive optical devices, including guided mode resonance (GMR) and plasmonic nanohole array (PNA) architectures, whose operation is typically dependent on the refractive index of constituent (passive) materials. GST-based devices provide a means to tune the optical response—through reversible index modulation—enabling wide wavelength operation and

narrow bandwidth tuning in the MWIR. Further design control is offered through altering the geometry of the nanostructure arrays / gratings. Moreover, the GST refractive index varies with composition ratio (XYZ; $Ge_xSb_yTe_z$) and indices of this thin-film layer can be fine-tuned, producing a continuum of resonance wavelengths with extremely narrow passbands. The tuning range can be increased outside the MWIR band into shorter (visible) and longer (long-wave infrared) regions by manipulating the angle of incidence, geometry, and the refractive index of additional materials.

We incorporate GST with three optical device architectures: conventional Fabry-Perot multilayer stacks, GMR-based filters, and PNA-based filters. These devices enable narrowband spectral resolution and 3~5µm wavelength tunability. Off resonance, the devices show near perfect absorption/reflection behavior. Through an optical stimulus – which changes the GST state from amorphous to crystalline – one can actively tune the filter with MHz speed (20~100 nanoseconds).

3.1. Multi-level Device

As a first proof-of-concept, we designed and fabricated a traditional Fabry-Perot multilayer filter using GST as a defect layer. This device was chosen as a baseline, as the operating principles and device response are well known, and incorporation of tunable materials such as liquid crystals has been previously demonstrated [6]. The fabricated device was designed with a resonance wavelength peak at 4.5 µm and consisted of twelve layers of Si (thickness of 329 nm) and Ge (thickness of 280 nm), with a 375 nm thick GST defect layer as the middle layer of the device. All films were deposited via magnetron sputtering at 7 mTorr working pressure and 50 W RF power. Once fabricated, the devices were characterized using FT-IR spectroscopy. First, the amorphous-phase response was measured. Subsequently, the device was heated using a hotplate to above the crystallization temperature of GST and measured again. A plot of the overlaid responses is shown in Figure 3. As is seen in the figure, the change in GST refractive index clearly results in a red-shift of the resonance peak. The reduction in transmission is attributed to the increased infrared absorption of the crystalline GST compared to the amorphous phase. Based on this successful proof of concept, GST was then implemented into two other device configurations which are discussed below.
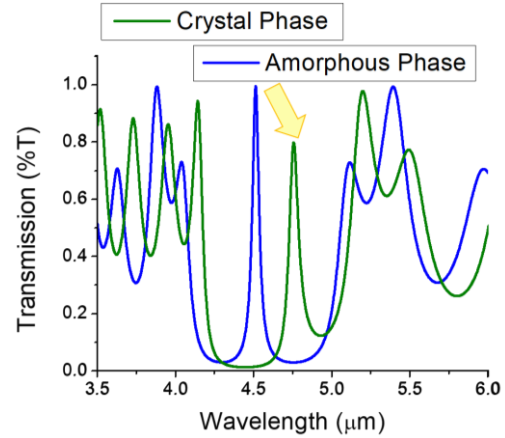

Figure 3. *Measured transmission response in amorphous and crystalline phases of the GST-based Fabry-Perot filter.*

3.2 Plasmonic Nanohole Array (PNA) Filter Device

In 1998, it was discovered by Ebbesen *et al*. that a periodic array of sub-wavelength nanoholes had an associated resonance at particular wavelengths, which gave rise to a phenomenon dubbed "extraordinary optical transmission" [17,18]. At a particular wavelength, the transmission of light through the array is several orders of magnitude higher than what is predicted by classical aperture theory. This is known to be attributed to surface plasmons excited at the interface of the metal holes and the surrounding dielectric and is explained in detail elsewhere [17]. The exact position of the resonance, and thus the center of the transmission passband, is governed by the metal and dielectric permittivities and the geometric period of the hole array.

When we consider this relation in the context of a square array of holes, we can obtain the position of the resonance wavelength given by the following equation:

$$\frac{\lambda_{res}}{\sqrt{l^2 + j^2}} = a_0 \sqrt{\frac{\varepsilon_m \varepsilon_d}{\varepsilon_m + \varepsilon_d}} \qquad (1)$$

Based on the above equation (1) for resonance wavelength, we can see that there are several degrees of freedom granted to the design of these hole array filters. Specifically, the choice of metal, dielectric, and hole periodicity allow for the precise placement of the resonance wavelength. Therefore, for the MWIR, material (index) selection and geometry are straightforward. In our design, Ag was selected as the metal material, and GST as our dielectric. A schematic of the design is shown below in Figure 4. CaF_2 was chosen as a substrate due to its high transparency across the MWIR.
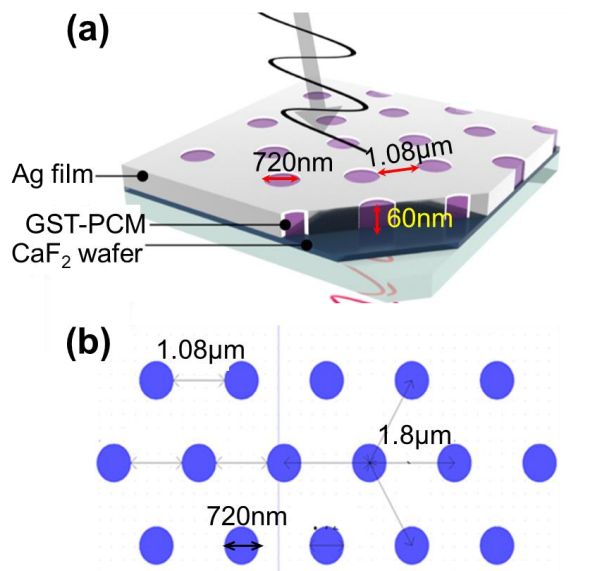
Figure 4. *Schematic of the PNA device showing (a) side view and (b) top view. GST is shown in purple.*

Finite-difference time domain (FDTD) simulations (Lumerical FDTD solutions) were used to investigate the optical properties of the device shown in Figure 5. Simulations were performed using linearly polarized light at normal incidence. Based on a target wavelength of 3 μm, a periodicity of 1.8 μm was chosen. The hole diameter was further optimized to be 0.4 times the array periodicity, in this case 720 nm. Figure 5 (a) shows simulated tuning behavior between amorphous and crystalline phases, (b) tuning performance as a function of GST refractive index, and array periodicity (c). Each parameter can be used to independently tune the transmission peak. Therefore, by combining the two tuning modalities, passbands of <200 nm can be tuned across 2~5 μm wavelength ranges, with near-zero transmissivity outside of the passband.
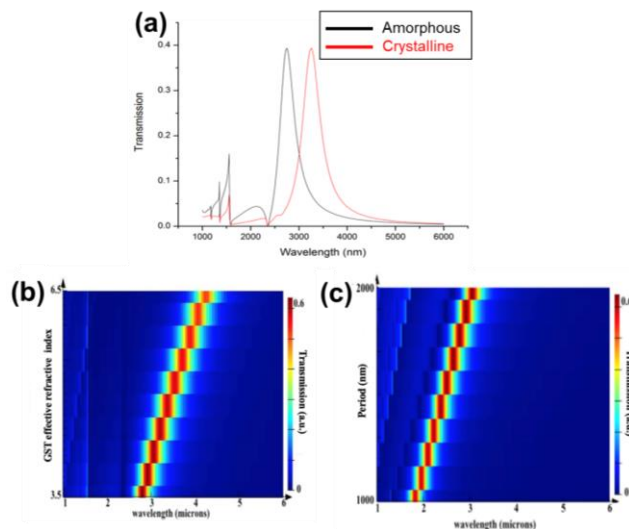

Figure 5. *(a) Transmission spectrum from a device based on the measured material dispersion for crystalline and amorphous GST phases. Simulated behavior of the GST nanohole array showing tuning capabilities via (b) GST refractive index and (c) array periodicity. By combining these two tuning methods, the full MWIR can be scanned. The passband in the above plots is 210 nm FWHM.*

Once designs were optimized through FDTD simulations, PNA devices were fabricated. Ag films of 60 nm thickness were patterned via lithography and subsequent chemical etching, and conformal deposition of 60 nm GST was performed via RF magnetron sputtering [19]. The periodicity of the fabricated array is 1.8 μm, and the hole diameter is 720 nm as shown in Figure 6 (a). Device dimensions matched well with designed values. Devices were characterized in terms of their optical transmission using FT-IR spectroscopy. Samples were characterized in the amorphous phase before experiencing a laser-induced phase change via a single laser pulse (Evergreen Nd: YAG-source of the laser light manufacture by Quantel laser). One exposed to the laser pulse (pulse duration = 100 ns, fluence = 30 mJ/cm^2), the GST was converted to crystalline phase and characterized again. After the crystalline phase transmission was measured, samples were irradiated by a second, shorter, higher energy laser pulse (pulse duration = 20 ns, fluence = 180 mJ/cm^2) in order to return the GST to the amorphous phase and were re-measured for a comparison. Figure 6 (b) shows the FT-IR results of the three phases. Upon re-entering the amorphous phase, the transmission spectrum is slightly shifted. This is attributed to a change in array geometry, as the heating may lead to expansion / deformation of the films' structure. However, the performance is consistent across five times heating/cooling cycles as shown plot of peak

wavelength vs. number of heating / cooling cycles in Figure 6 (c). The results suggest that the design is robust and appropriate for switchable passband applications.
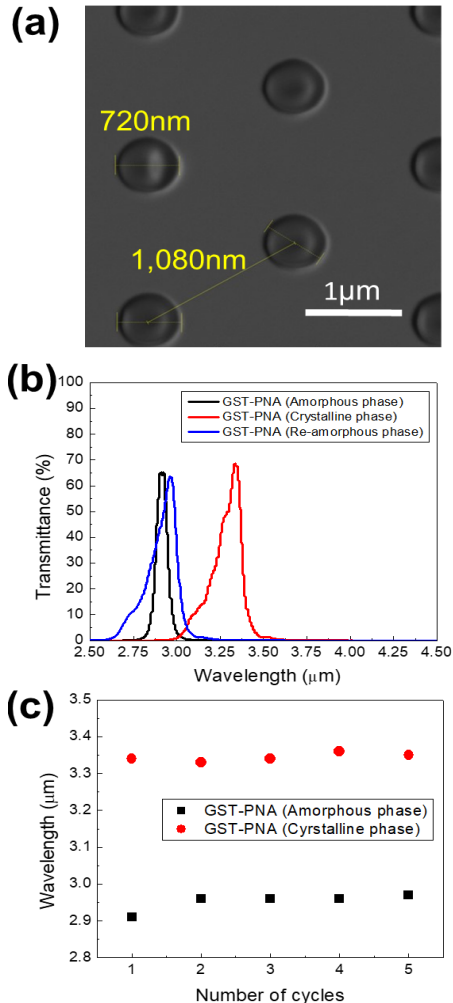

Figure 6. *(a) SEM image of fabricated PNA device (b) FT-IR data showing the temperature-tunable passbands of the nanohole array device. Results match reasonably well with simulated data. The widened passband in the case of re-amorphous samples is possibly due to material expansion (and thus a shift in array geometry) after heating. (c) Position of peak resonance wavelength as a function of the number of heating/cooling cycles showing consistent performance across multiple phase changes.*

3.3 Guided Mode Resonance (GMR) Filter Device

Guided mode resonance devices are essentially a combination of a diffraction grating and waveguide. The grating is realized by either a physical (e.g. etched) structure or by a periodic modulation of the layer refractive indices. A schematic of each of these variations of a GMR device is shown in Figure 7.
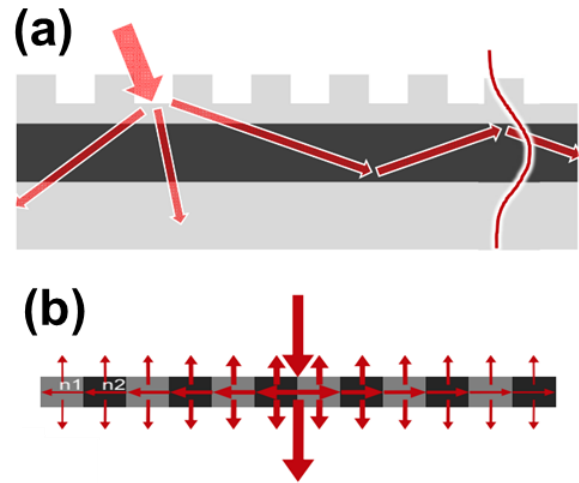

Figure 7. *Schematics depicting the operation concept of GMR devices where (a) the grating and waveguide are separate and (b) single layers. Incident light matching the resonance condition is diffracted by the grating and guided by the core. The guided mode will the "leak" from the waveguide layer and interfere with incident light, producing a filtering response.*

Incident light satisfying the phase matching condition of the coupled grating/waveguide structure will be guided in the waveguide, while the rest of the light will be transmitted or reflected. As the guided mode propagates, it will experience some loss as it slowly "leaks" from the waveguide. This leaked light will interfere with the incident light or reflected light, depending on which regime the device operates in, producing a filtering response.

As the GMR device resonance depends on the angle of incidence, device period, and refractive index, we tune the device resonance by modulating the refractive index of the constituent grating materials. We integrate GST into a customized GMR filter in which we can actively control its refractive index and thus in effect enable tunability across the MWIR spectrum. The "effective index" of the grating changes the resonance properties, as well as the passband width. Thus, through either an applied electric field or optically induced heating—which changes the GST state from amorphous to crystalline—we can actively tune the filter to provide a resonant filtered wavelength.

Figure 8 shows transmission spectral of the simulated GMR device. A similar FDTD environment was used as in the PNA device. The device simulated is an index modulated structure where the grating periodicity comes from a variation between CaF_2 and GST, with a period of 3.1 µm and a GST filling factor of 0.75. The GST/CaF_2 layer is taken to be 400 nm thick,

and the incident light is linearly polarized in the direction perpendicular to the grating period.

The device shows a 10 nm transmission bandwidth with perfect out-of-band reflection across an 800 nm bandwidth in the MWIR. This represents a bandwidth of only 111 GHz, and a resonance Q-factor of ~520. It should be noted that this device design may be improved and greater out-of-band reflection is possible through careful optimization of the grating layer of the guided mode resonance structure.
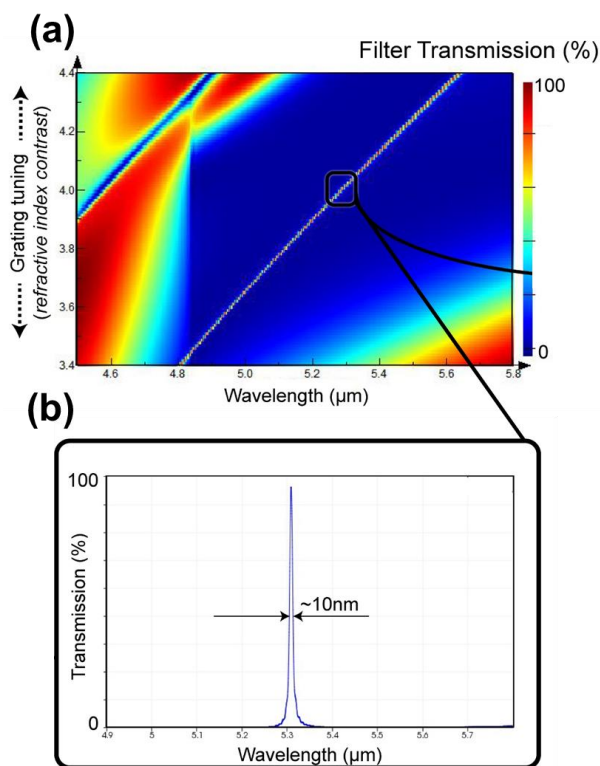

Figure 8. (a) FDTD simulated behavior of the guided mode resonance showing tuning capabilities via GST refractive index changes and (b) transmission spectra with 10nm bandwidth at 5.3 μm wavelength

4. GST-based toolbox

There are numerous phase-change alloys are existed. The most widely used and well researched is an alloy of $Ge_2Sb_2Te_5$ (used here) for the use in re-writable optical disc formats and the PRAM. For specific applications with targeted wavelength bands, we can select and combine various alloys with modified device designs to create unique tunable filter toolbox. For example, the refractive index of $Ge_2Sb_2Te_6$ is approximately double when crystallized over the wavelength range of 2 – 12 μm, providing excellent tunability. The amorphous phase is effectively transparent from ~1.5 μm onwards, and although the crystalline phase is substantially more absorbing, in mid and long wave infrared, it remains useable in transmission devices provided thickness are kept low [3]. It is also possible to incorporate other atoms into the PCM alloy in order to increase the transparency of the crystalline state [20]. As long as the PCM is transparent to the wavelength of interest, the device can also be scale to other wavelength ranges including the visible wavelength range.

5. MISSE (Materials International Space Station Experiment) for space applications

In order to evaluate the performance and lifetime of tunable MWIR filters for space applications, the PCM and resultant filters must be exposed to a relevant Low Earth Orbit (LEO) space environment that allows the effects of thermal cycles, hard vacuum, atomic oxygen scrubbing, radiation, and contamination to be observed. (1) Atomic oxygen would affect optical properties of filter as released molecules could re-deposit on the MWIR filter surface. (2) UV exposure under high vacuum might lead to optical property changes of the filter by changing the compositions of the PCM and material heating. (3) The extreme heat and cold thermal cycle might degrade the filter efficiency. These cyclic temperature variations are -120 °C to +120 °C, and high solar absorptance with low infrared emittance of the filter materials will contribute to greater temperature swings. Testing and qualification of MWIR filters exposed to these extreme conditions at ISS would provide data to enable the manufacturing of long-term reliable components used on space, satellite, and spacecraft. We proposed the MISSE-14 opportunity with either Wake or Zenith carrier orientation for studying UV exposure and solar illumination effects for the tunable filters [21]. Both the solar cycling data and the UV exposure data from the orientations are going to be useful for the future science measurement instrumentation.

6. Conclusions

The MWIR spectrum contains a wealth of invaluable information: from the spectral 'fingerprint' of many chemical species, with applications in remote sensing, to radiant thermal signatures, utilized in astronomical and military imaging systems. For accurate next-generation MWIR spectral imaging applications, the ability to extract the maximum amount of information with high-resolution, MHz tuning speeds, with reduced size and mass, is paramount. PCM offers the advantages of MHz switching speed, up to 10^{15} switching robustness, and scaling potential. This characteristics of the PCM are highly relevant ultrafast and active tuning optical device

applications with integrated known passive optical device design.

We have designed, simulated, and experimentally demonstrated actively tunable MWIR transmission filters based on GST-PCM, incorporated into a GMR (<10 nm resolution) and PNA (2~5 µm wavelength tenability). By altering the crystal phase of the GST-PCM film, active tuning of the filter devices can be achieved without the use of any moving parts. Through design, the device can be scaled to other wavelength ranges so long as the PCM selected is transparent in the wavelength region of interest. Using discriminated narrowband signals and multi-spectral / broad wavelength tunability, the PCM-MWIR filter will be able to extract the maximum amount of useful information within the atmosphere for remote Earth sensing measurements. Through an optical stimulus – which changes the GST state from amorphous to crystalline – one can actively tune the filter with MHz speed (20~100 ns). This technology exhibits operational speeds orders of magnitude faster than current airborne-based sensors. Moreover, it enables affordable SmallSat-based MWIR instrumentation which is complimentary to other observation systems.

Acknowledgements

References

[1] C. S.-C. Yang, E.E. Brown, E. Kumi-Barimah, U.H. Hommerich, F. Jin, S.B. Trivedi, A.C. Samuels, A.P. Snyder, Mid-infrared, long wave infrared (4-12µm) molecular emission signatures from pharmaceuticals using laser-induced breakdown spectroscopy, Appl. Spectrosc. 68 (2014) 226–23.

[2] D. A. Cremer and L. J. Radziemski, Handbook of Laser-induced Breakdown Spectroscopy, 2nd ed. Wiley, 2013.

[3] L. Trimby, A. Baldycheva, C.D. Wright, Phase change band-pass filters for multispectral imaging, Proc. Of SPIE 2018, 10541.

[4] A. Rogalski, Infrared detectors: an overview, Infrared Physics & Technology 43 (2002) 187-210.

[5] M. Ebermann, N. Neumann, K. Hiller, M. Seifert, M. Meinig, and S. Kurth, Tunable MEMS Fabry-Perot filters for infrared microspectrometers: A review, Proc. SPIE 9760 (2016) 97600H-1.

[6] H. Zhang, A. Muhammad, J. Luo, Q. Tong, Y. Lei, Z. Zhang, H. Sang, and C. Xie, Electrically tunable infrared filter based on the liquid crystal Fabry-Perot structure for spectral imaging detection, Appl. Opt. 53 (2014) 5632-5639.

[7] M. Wuttig, D. Lusebrink, D. Wamwangi, W. Welnic, M. Gilleben, and R. Dronskowski, The role of vacancies and local distortions in the design of new phase-change materials, Nature Materials, 6 (2007) 122-128.

[8] M. Wuttig, H. Bhaskaran, and T. Taubner, Phase-change materials for non-volatile photonic applications, Nature Photonics, 11 (2014) 465-476.

[9] W. Bai, P. Yang, J. Huang, D. Chen, J. Zhang, Z. Zhang, J. Yang, and B. Xu, Near-infrared tunable metalens based on phase change material Ge2Sb2Te5, Scientific Report 9 (2019) 1-9.

[10] A.R. Nehir, C. Kiemle, M.D. Lebsock, G. Kirchengast, S.A. Buehler, U. Lohnert, G.-L. Liu, P.C. Hargrave, M. Barrera-Verdejo, D.M. Winker, Emerging technologies and synergies for airborne and space-based measurements of water vapor profiles, Surv Geophys 38 (2017) 1445-1482.

[11] 2017 Decadal Survey, https://science.nasa.gov/earth-science/decadal-surveys

[12] The SCIFLI (Scientifically Calibrated In Flight Imagery) team, based at NASA Langley Research Center, https://scifli.larc.nasa.gov/

[13] Ovshinsky, U.S. Patent 3,271,591, 1966.

[14] P. Guo, A.M. Sarangan, and I. Agha, A Review of Germanium-Antimony-Telluride Phase Change Materials for Non-Volatile Memories and Optical Modulators, Appl. Sci. 9(3) (2019) 530.

[15] P. Hosseini, C.D. Wright, and H. Bhaskaran, An optoelectronic framework enabled by low-dimensional phase-change films, Nature 511 (2014) 306-211.

[16] K.B. Borisenko, K.Shanmugam, B.A.O. Williams, P. Ewart, B. Gholipour, D.W. Hewak, R. Jussain, T Javorfi, G. Siligardi, and A.I. Kirkland, Photo-induced optical activity in phase-change memory materials, Sci. Report, 5 (2015) 8770.

[17] T.W. Ebbesen, H.J. Lezec, H.F. Ghaemi, T. Thio, and P.A. Wolff, Extraordinary optical transmission through sub-wavelength hole arrays, Nature 391 (1998) 667-669.

[18] C. Genet and T.W. Ebbesen, Light in tiny holes, Nature 445 (2007) 39-45.

[19] H.J. Kim, T. Johns, Active optic component development: unique capabilities within the advanced measurements and data systems branch at NASA LaRC, NASA Technical Interchange Meeting on Active Optical Systems for supporting Science, Exploration, and Aeronautics measurements needs, USRA Headquarters, July 31-August 2, 2018.

[20] Y. Zhang, J.B. Chou, J. Li, H. Li, Q. Du, A. Yadav, S. Zhou, M.Y. Shalaginov, Z. Fang, H. Zhong, C. Roberts, P. Robinson, B. Bohlin, C. Rios, H. Lin, M Kang, T. Gu, J. Warner, V. Liberman, K. Richardson, and J. Hu, Extreme broadband transparent optical phase change materials for high-performance non-volatile photonics, Nature Comm. 10 (2019), 4279.

[21] MISSE: Testing materials in space https://www.nasa.gov/centers/langley/news/factsheets/MISSE.html